Trace element composition and cathodoluminescence properties of southern African kimberlitic zircons

E. A. Belousova[1], W. L. Griffin[1,2] AND N. J. Pearson[1]

[1] National Key Centre for Geochemical Evolution and Metallogeny of Continents, School of Earth Sciences, Macquarie University, Sydney, NSW 2109, Australia
[2] CSIRO Exploration and Mining, P.O. Box 136, North Ryde, NSW 2113, Australia

ABSTRACT

Zircon frequently occurs as a minor mineral in kimberlites, and is recognised as a member of a suite of mantle-derived megacryst minerals. Cathodoluminescence (CL) microscopy and laser ablation ICPMS analysis were used to study the internal structure and chemical composition of zircon crystals from southern African kimberlites. Zoning revealed by CL ranges from fine oscillatory to broad homogeneous cores and overgrowths. The ICPMS data show that kimberlite zircons have distinctive trace element contents, with well defined ranges for *REE*, Y, U, Th, P and some other trace elements. Both low *REE* contents (ΣREE < 50 ppm), and distinctive chondrite-normalised *REE* patterns with low and flat *HREE* are characteristic of kimberlite zircons. Samples or zones with yellow CL have higher Th, U, Y, and *REE* than those with blue-violet CL. Variations in the concentrations of a range of trace elements lead to different amounts of lattice defects, creating the possibility for different levels of direct excitation of luminescence centres, and therefore different CL colours. The distinctive CL and compositional features described here can rapidly identify kimberlite zircons in prospecting samples taken during exploration for kimberlite bodies.

Introduction

ZIRCON is a common mineral in a wide range of rocks ranging from mafic to felsic in composition. It is more widely distributed in granitoid rocks and gneisses. Less frequently, it occurs in mafic and ultramafic rocks, and zircon is found as a minor phase in many kimberlites. Usually, the zircon content of kimberlites is about 1 gram per ton or less, but in some cases it is up to 25 g/t (Bultfontein, Rietfontein) or more than 50 g/t (Orapa: Kresten *et al.*, 1975; Yakutian kimberlites: Krasnobayev, 1979). Despite its low abundance, zircon is easily concentrated, due to its high density and its X-ray fluorescence properties.

The frequent occurrence of zircon in kimberlites suggests that, by finding specific characteristic features of kimberlite zircons, it may be used as an indicator mineral during diamond exploration. This work has been done to characterize kimberlite zircons using their geochemical, cathodoluminescence and morphological features. Fifty-one zircon grains from 12 kimberlite pipes in southern Africa have been studied for this purpose (Table 1).

The investigated zircons, with grain size from 0.5 to 6 mm, have been prepared as thick (about 100 μm) polished sections or as grains mounted in epoxy. They are assumed to be part of the mantle-derived megacryst assemblage, which includes olivine, low-Cr garnet, pyroxenes and ilmenite. Zircons in the Monastery Mine kimberlite are known to be intergrown with megacrystic (iron-rich) olivine, ilmenite and phlogopite, which formed late in a fractional crystallization sequence (Moore *et al.*, 1992).

TABLE 1. Laser ablation ICPMS analysis of kimberlite zircons. Representative data selected from 168 analysis

Sample no.	Location	CL colour	P	Ti	Mn	Fe	Ga	Sr	Y	Nb	Sn	Ba	La	Ce
ROM-179-1	Monastery Mine	blue	78.6	15	<1.0	<17	<0.5	<0.1	17.3	3.6	<0.7	<0.1	<0.05	0.6
ROM-179-2	Monastery Mine	yellow	71.6	15	<1.2	<13	<0.4	0.1	49.4	3.2	<0.7	<0.09	<0.07	1.0
ROM-179-3	Monastery Mine	blue	60.5	16	<1.5	20	<0.6	0.5	16.1	2.3	<0.5	0.4	<0.07	0.7
kn279(12) 1	Monastery Mine	pink	50.4	34	<0.3	<5	0.2	0.1	54.0	3.1	0.3	<0.02	0.33	0.8
kn279(12) 2	Monastery Mine	pink	39.9	29	<0.2	<3	<0.1	0.0	46.5	2.5	0.3	<0.07	<0.01	0.7
kn279(12) 4	Monastery Mine	pink	36.9	23	<0.9	<5	<0.1	0.1	39.9	2.2	0.2	<0.02	<0.02	0.6
M28(8) 1	Dyke 170	blue	56.6	23	2.9	<9	1.9	2.1	20.6	3.7	2.3	0.4	0.79	1.6
M28(8) 2	Dyke 170	yellowish	49.0	24	1.0	<8	<1.2	0.1	46.7	2.5	0.7	<0.7	0.05	1.4
M31-1	Sekameng/	blue	61.7	15	<1.0	11	<0.7	0.2	28.9	2.9	0.4	<0.1	<0.25	0.9
M31-2	Butha Buthe	yellowish	78.6	15	<0.9	<12	<0.6	0.2	38.5	3.8	<0.6	0.9	0.07	1.3
M30(10) 1	Mothae	blue	47.3	24	<0.6	<10	0.7	0.2	44.3	3.0	0.6	0.4	<0.04	1.1
M30(10) 2	Mothae	blue	35.2	22	<0.6	<5	0.5	0.2	42.4	3.0	<0.6	<0.2	0.07	0.8
M30(10) 3	Mothae	blue	49.6	24	<1.2	<8	<0.3	0.4	50.2	3.5	0.7	0.2	0.11	1.0
M42(2) 1	Kao 1	blue	49.1	14	<1.3	<17	<0.6	<0.4	10.7	1.7	1.8	<0.3	<0.19	1.1
M42(2) 2	Kao 1	yellowish	71.8	20	1.9	<21	<0.5	0.1	22.3	2.7	0.8	0.4	<0.05	0.8
M42(2) 3	Kao 1	blue	68.5	19	<0.9	<14	<0.4	0.1	25.1	2.7	0.6	<0.05	<0.05	0.6
M42(2) 4	Kao 1	yellow	110.4	28	1.4	40	2.3	0.8	75.3	11.2	1.0	0.8	<0.08	1.5
M27-1	Lemphane	yellowish	76.6	23	<1.2	<18	0.8	<0.1	67.9	7.3	<0.9	<0.06	<0.15	1.4
M27-2	Lemphane	blue	77.8	16	<2.1	<13	1.6	0.7	50.9	3.9	2.2	0.6	<0.09	1.1
M27-3	Lemphane	yellow	46.1	11	<1.1	<11	<0.4	0.2	51.9	2.3	2.3	0.2	0.35	1.5
M101-1	De Beers Mine	blue	93.6	27	<1.9	<15	<0.6	<0.1	17.9	2.8	1.1	<0.08	<0.11	0.6
M101-2	De Beers Mine	blue	92.5	31	<0.9	<17	<0.6	<0.1	17.0	2.4	<0.5	<0.1	<0.08	0.8
M101-3	De Beers Mine	blue	96.3	26	<1.0	<13	<0.5	0.4	19.2	2.5	0.5	<0.08	0.06	0.7
M102-1	Bultfontein	yellow	32.4	17	<0.4	21	<0.15	0.1	74.6	2.7	0.3	0.3	0.02	1.5
M102-2	Bultfontein	yellow	20.9	15	0.3	<4	0.3	0.1	56.5	1.7	0.3	<0.1	0.09	1.1
M102-3	Bultfontein	yellow	28.7	17	<0.4	<4	0.5	0.3	73.8	2.3	0.8	0.4	0.12	1.7
M103-1	Wesselton	yellow	50.7	41	2.8	93	0.3	0.4	59.6	<1.96	228	0.8	0.15	2.5
M103-2	Wesselton	yellow	26.7	13	<0.3	7	0.2	0.2	56.0	1.9	0.5	0.1	0.06	1.9
Average for all kimberlite zircons			65.8	21			1.1	0.8	38.8	3.6	5.0	0.9	0.37	1.3
		St. dev.	20.9	5			0.5	3.1	18.7	2.1	27.2	2.9	1.58	2.0
AVERAGE for bluish CL			63.8	20			1.2	0.8	27.1	3.3	2.1	1.1	0.40	1.1
		St. dev.	15.9	5			0.4	0.4	14.2	0.8	0.6	0.3	0.15	0.3
AVERAGE for yellow CL			56.5	21			1.1	0.2	54.4	3.5	12.8	0.4	0.12	1.2
		St.dev	18.4	5			0.7	0.2	11.5	1.8	52.2	0.3	0.08	0.4

TABLE 1 (contd). Laser ablation ICPMS analysis of kimberlite zircons

Sample number	Pr	Nd	Sm	Eu	Gd	Dy	Ho	Er	Yb	Lu	Hf*	Ta	Pb	Th	U	U**
ROM-179-1	<0.03	<0.4	<0.3	0.12	0.8	2.2	0.7	2.6	3.0	0.5	1.41	4.3	<0.3	1.8	8.0	
ROM-179-2	<0.05	0.5	0.6	0.32	2.8	7.1	1.8	6.2	7.6	1.2	1.27	2.8	<0.3	3.6	11.0	
ROM-179-3	0.06	<0.3	0.5	<0.15	0.6	1.7	0.5	1.9	2.9	0.5	1.31	2.2	<0.3	1.5	6.5	
kn279(12) 1	0.04	0.2	0.5	0.39	2.7	7.2	1.9	6.4	7.2	1.3	1.40	2.5	<0.08	3.5	9.6	8.0
kn279(12) 2	0.01	0.4	0.6	0.39	2.5	6.3	1.7	5.8	6.5	1.1	1.39	2.1	0.04	3.2	8.2	
kn279(12) 4	0.01	0.2	0.6	0.33	2.3	5.0	1.5	4.9	5.3	0.9	1.35	1.8	<0.06	2.7	7.1	
M28(8) 1	0.67	1.2	0.6	<0.89	1.5	3.0	1.1	2.6	3.4	0.9	1.62	2.8	2.5	2.0	9.1	10.9
M28(8) 2	0.14	0.5	0.7	0.52	3.0	6.2	1.8	5.4	7.1	1.2	1.32	2.0	0.6	3.0	7.6	
M31-1	0.53	<0.4	0.6	<0.89	1.0	3.2	0.9	3.3	4.4	0.7	1.46	2.9	<0.2	2.2	11.1	11.4
M31-2	<0.47	0.3	0.4	0.34	1.8	4.3	1.4	4.9	7.2	1.3	1.50	4.2	<0.3	3.2	12.7	
M30(10) 1	<0.07	0.4	0.7	0.46	2.9	6.1	1.6	5.6	6.3	1.1	1.49	2.6	0.6	4.2	10.4	8.7
M30(10) 2	0.09	0.4	0.6	0.52	2.7	6.0	1.6	5.4	5.8	1.1	1.38	2.3	<0.2	3.7	9.5	
M30(10) 3	0.16	0.3	0.7	0.45	3.1	6.9	1.9	6.2	8.0	1.3	1.66	2.8	<0.2	4.4	11.6	
M42(2) 1	<0.14	<0.7	<0.5	<0.37	<0.5	0.8	<0.2	1.2	1.8	0.2	1.31	1.5	<0.5	0.8	6.7	18.1
M42(2) 2	0.19	0.3	<0.3	0.15	1.0	3.2	0.9	2.4	4.2	0.7	1.41	2.5	<0.5	2.2	8.0	
M42(2) 3	0.04	0.2	0.4	0.15	1.1	2.5	0.9	3.1	4.0	0.7	1.44	3.1	0.4	2.3	8.9	
M42(2) 4	0.07	0.6	0.7	0.51	2.9	9.6	2.8	9.3	10.8	1.8	1.44	9.8	0.3	13.5	38.1	
M27-1	0.8	<0.4	0.5	0.42	3.4	7.5	2.3	8.5	11.8	2.0	1.32	6.2	<0.4	6.4	25.3	
M27-2	0.27	<0.3	0.5	0.34	1.9	5.7	1.6	6.0	7.6	1.6	1.25	4.6	0.5	3.7	16.2	12.2
M27-3	0.15	0.7	0.6	0.56	3.1	7.7	1.8	7.0	8.6	1.3	1.02	2.5	1.7	3.6	10.8	
M101-1	<0.15	<0.5	<0.6	<0.17	0.9	2.2	0.6	2.2	2.4	0.3	1.46	1.9	<0.3	1.5	7.0	6.7
M101-2	0.05	<0.2	<0.4	0.27	0.7	2.3	0.7	2.1	2.2	0.5	1.36	1.6	<0.3	1.4	6.8	
M101-3	<0.03	<0.2	<0.4	0.2	1.2	2.4	0.7	2.0	2.6	0.5	1.51	1.9	0.2	1.5	7.3	
M102-1	0.07	0.8	1.2	0.64	3.8	9.3	2.7	9.7	12.7	2.4	1.02	2.2	1.0	8.7	20.8	13.8
M102-2	0.09	0.6	0.8	0.58	2.7	7.1	2.1	7.2	9.5	1.7	0.91	1.7	0.7	6.4	15.4	
M102-3	0.21	0.9	1.3	0.81	3.6	9.5	2.7	9.8	12.6	2.3	1.05	2.3	1.5	8.6	22.1	
M103-1	0.11	0.5	1.1	0.66	3.3	7.8	2.2	7.4	10.4	2.2	0.97	1.4	12.3	12.2	27.1	22.1
M103-2	0.06	0.5	0.9	0.59	3.1	7.0	2.0	7.2	10.2	2.0	0.86	1.2	1.2	11.2	25.0	
Average for all	0.42	0.7	0.9	0.67	2.2	5.2	1.5	5.0	6.1	1.1	1.39	3.0	1.9	3.3	10.9	
St.dev	1.81	1.2	1.3	1.56	1.3	2.6	0.8	2.3	2.8	0.6	0.17	1.2	5.3	2.1	5.5	
Average for bluish CL	0.50	0.7	0.8	0.58	1.5	3.5	1.1	3.5	4.5	0.8	1.43	2.8	1.3	2.2	8.8	
St. dev	0.15	0.3	0.2	0.32	0.9	2.0	0.5	1.7	2.0	0.3	0.15	0.7	1.1	1.1	2.4	
Average for yellow Cl	0.16	0.6	0.9	0.54	2.9	7.2	2.0	6.8	8.3	1.5	1.27	3.0	1.3	5.0	14.0	
St. dev	0.16	0.2	0.3	0.15	0.7	1.6	0.4	1.5	2.0	0.4	0.20	1.6	2.5	2.9	7.0	

† All concentrations are given in ppm

* Hf (wt%) has been analysed by electron microprobe and used as an internal standard. concentrations are given in wt.%

** Fission track analyses data (Kresten, unpub. data)

Morphological and cathodoluminescence properties

The morphology of the kimberlite zircon grains does not show clearly defined features peculiar to the zircon of kimberlites. They are characterized by the almost complete absence of crystal faces, and are usually rounded to subrounded. The colours vary from colourless to reddish brown, and honey-yellowish colours are most abundant. Some zircons are covered with a whitish coating (green fibrous rims on Fig. 1*e*), which has previously been identified as a mixture of monoclinic (baddeleyite) and tetragonal zirconia (Kresten *et al.*, 1975). The most distinctive morphological feature of the kimberlite zircons studied here is their large grain size which typically is several millimetres, while in most other igneous or metamorphic rocks zircons seldom reach more than 0.05–0.3 mm. However, Kresten *et al.* (1975) and Lyakhovich (1996) have reported small euhedral grains of zircon in kimberlites.

A cold cathode luminescence stage (CITL, Model CCL 8200 mk3) mounted on a petrographic microscope has been used to study the internal structure within zircon crystals. This has the advantage of showing features which are not visible in transmitted or reflected light. Kimberlite zircons show bluish, yellowish and pinkish cathodoluminescence (CL) colours, with bluish hues predominating, while all crustal zircons examined thus far in our laboratory have yellowish CL. Many of the investigated crystals show evidence of complicated growth histories in the form of complex zoning patterns or overgrowths. The zoning patterns revealed by CL can be divided into three distinct groups:

(i) thin oscillatory zones which vary in thickness from about 1 to 20 µm, rarely up to 50 µm. Different zones may vary only in intensity of colour, or may have different hues (Fig. 1*a,b*);

(ii) thick bands or well distinguishable cores and overgrowths with well defined straight boundaries (Fig. 1*c*);

(iii) broad, almost featureless bands and irregularly shaped areas with curved margins (Fig. 1*d,e,f*) that may reflect deformation at high pressure (Kresten *et al.*, 1975; Lyakhovich, 1996).

Analytical technique

The Cameca SX-50 Electron Microprobe at Macquarie University has been used for determi-

nation of major elements in zircon: Zr, Si and Hf. The main reason for this analysis was to determine Hf heterogeneity, as this element is used as the internal standard for further trace element determination by laser ablation ICPMS. An accelerating voltage of 15 kV and a beam current of 20 nA was used for all analyses. The spatial resolution of the electron microprobe was about 2 µm. The detection level for Hf was 0.09% with a precision of 3% relative standard deviation at 1% HfO_2. The PAP matrix correction routine has been applied.

Trace elements have been analysed by laser ablation ICPMS at Macquarie University. Detailed descriptions of instrumentation, analytical and calibration procedures are given by Norman *et al.* (1996). The UV laser ablation microprobe is coupled to a Perkin-Elmer Elan 5100 ICPMS. Detection limits are typically less than 0.3 ppm for the *REE*, Y, P, Th and U. All analyses have been done with a pulse rate of 4 Hz and a beam energy of 1 mJ per pulse, producing a spatial resolution of 30–50 microns in the zircons. Quantitative results for 28 elements were obtained through calibration of relative element sensitivities using an external NIST-610 glass standard, and normalization of each analysis to the electron-probe data for Hf as an internal standard. The precision and accuracy of analysis are ± 2–5%, and up to ± 10% for Fe and for other elements with concentrations less than 1 ppm.

Results

Table 1 shows representative trace element data selected from 168 analyses of southern African kimberlite zircons. Because of the complex internal structure revealed by CL study in most of the grains, several analytical points have been analysed in each crystal to relate the variations in chemical composition with variations in cathodoluminescence properties. Figure 2 shows chondrite-normalized values of analysed trace elements arranged in order of their ionic radius. This organisation illustrates the principle that the most abundant cations of each valency state are those with ionic radii closest to Zr–Hf (Jensen, 1973). In addition to the averaged data for all southern African kimberlite zircons (Table 1), chondrite-normalized values of averaged concentrations for zircons from some other crustal sources are given for comparison (Fig. 2, Table 2). Samples 61.308 and 91500 are zircon
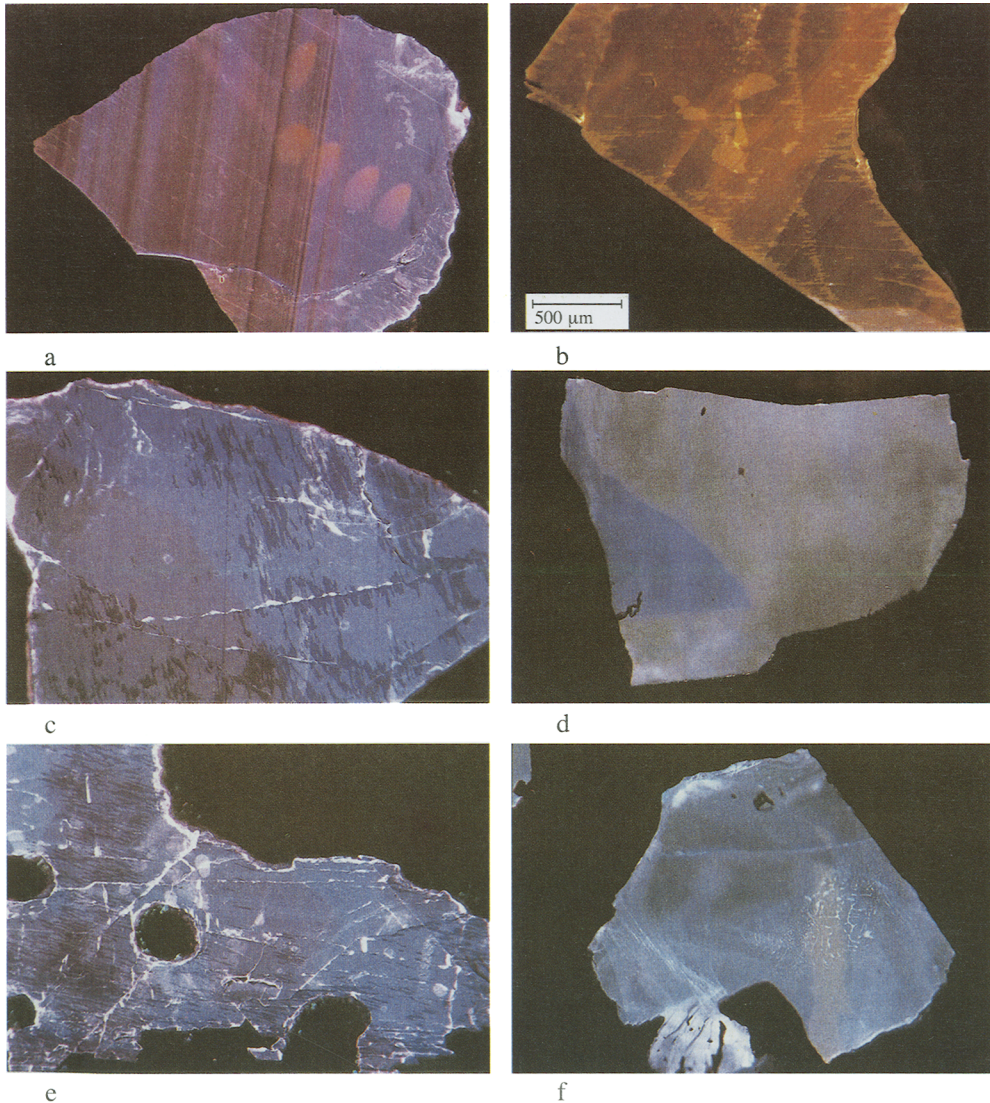
FIG. 1. Cathodoluminescence images of kimberlitic zircons.

standards described by Weidenbeck *et al.* (1995). Data for zircon inclusions in corundum mega-crysts plotted here have been taken from Guo *et al.* (1996). *REE* patterns of those samples are shown in Fig. 3.

The major components (Si, Zr, Hf) show no principal differences from the range found in crustal zircons. The Zr/Hf ratio of kimberlitic zircons varies between 30 and 41 with an average of 36, consistent with the data of Kresten *et al.*(1975), who found an average Zr/Hf ratio of 38, similar to that seen in crustal zircons. For example, the Zr/Hf ratio of zircons from granitoid rocks of the New England Batholith (eastern Australia) ranges from 21 to 42 with an average of 32 (Belousova, unpub. data). However, the trace-
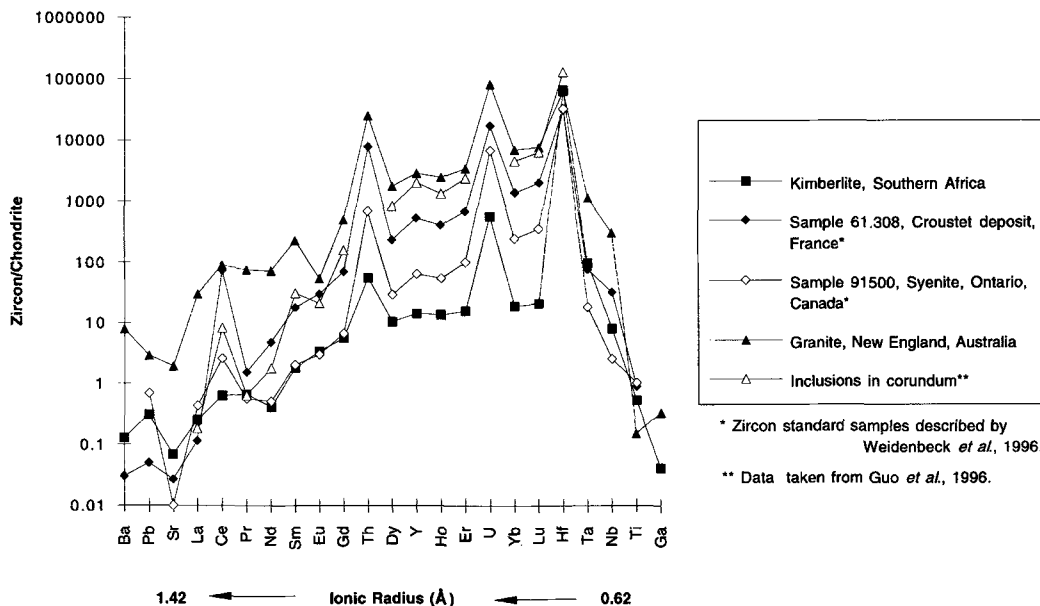
FIG. 2 Trace element patterns of zircons from different sources: chondrite-normalized abundances versus ionic radius. IR data from Shannon (1976).

element compositions show significant differences in comparison to zircons of any other origin for which data are available.

Phosporus ranges from 20 to about 110 ppm for kimberlite zircons, while it varies from hundreds to thousands of ppm in zircons from granitoid rocks (Fig. 4). Yttrium contents are not more than 80 ppm and mainly range from 20 to 60 ppm, whereas in crustal zircons Y may reach percent-level concentrations (Fig. 2). Detection limits for manganese and iron are rather high, and few points give values above the MDL. Tantalum and niobium show a strong positive correlation (Nb/Ta = 1.18 ± 0.21 (1 std.
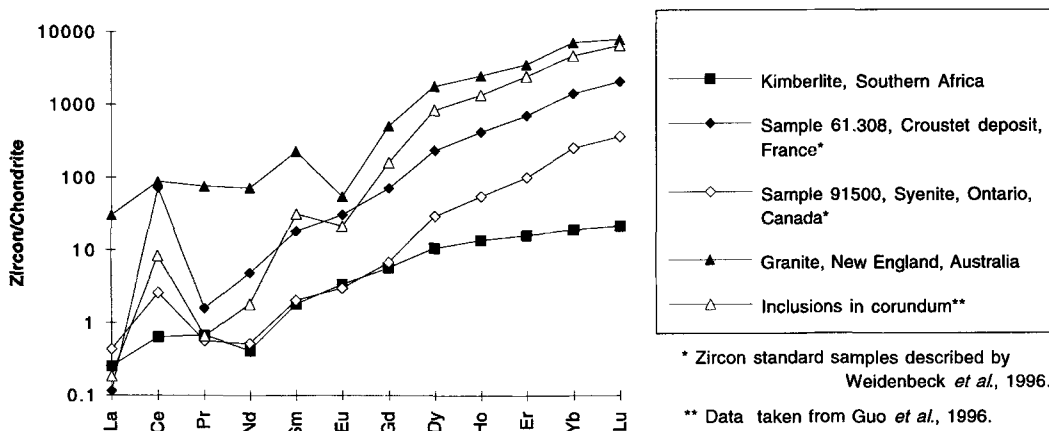
FIG. 3. Rare earth element patterns of zircons from different sources.

TABLE 2. Laser ablation ICPMS analysis of zircons from different sources (averaged data for several analytical points)[†]

Elements	Sample 61308 Croustet deposit France		Sample 91500 Syenite Ontario, Canada		Sample NEB291 Granite Ebor, Australia	
	Conc.	St. dev.	Conc.	St. dev.	Conc.	St. dev.
P					2770	2190
Sc					576	351
Ga					6.4	3.9
Sr	0.3	0.2	0.1	0.04	59	49
Y	1220	599	146	22	14500	11300
Nb	12.5	9.3	1.0	0.1	318	241
Ba	0.1	0.04			65	50
La	0.05	0.02	0.2	0.1	29.4	21
Ce	69	56	2.5	0.5	162	107
Pr	0.2	0.2	0.1	0.1	25.7	21
Nd	3.4	3.4	0.4	0.1	133	114
Sm	4.2	3.4	0.5	0.2	126	103
Eu	3.0	2.2	0.3	0.1	6.2	2.8
Gd	21.7	14.5	2.1	0.3	338	269
Dy	90	51	11.2	2.1	1570	1250
Ho	35.7	17.9	4.7	0.6	456	341
Er	177	82	25.3	3.6	1850	1390
Yb	350	141	62	7	3520	2580
Lu	78	25	13.9	1.8	553	395
Lu*	73−101		11−13			
Hf	5658*		5895*		13750	7660
Ta	2.0	1.0	0.5	0.1	38.5	46
Ta**	2.66−3.37		0.32−0.56			
Pb	0.2	0.1	2.5	0.7	17.2	11
Th	338	330	29.8	4.7	1790	1290
Th**	283−461		39.3−41.7			
U	216	153	85	14	1890	1630
U**	220−267		85.4−97.8			
Number of analyses	4		4		7	

[†] All concentrations are given in ppm.
* Lu-Hf isotope dilution data (Wiedenbeck, 1995)
** Data obtained by INAA (Wiedenbeck, 1995)

dev)) over a concentration range from 1 to 11.2 ppm Nb. The correlation between Nb and Ta strongly suggests that the low Nb/Ta is real, rather than an artefact of analysis. If the valency of Nb and Ta is 5^+, then their ionic radii are similar (Shannon, 1976), giving these elements equal potential to enter the zircon lattice. Therefore, the Nb/Ta ratio in zircons should reflect the Nb/Ta ratio of their environment. However, Kabanova et al. (1982) reported high (average 16.8) Nb/Ta ratios for kimberlites and the chondritic ratio is about 14 (Taylor and McLennan, 1985). There are at least two explanations for the low Nb/Ta ratio in kimberlitic zircons. It could be explained by the ability of Nb to form its own minerals in alkaline, ultramafic environments, whereas Ta remains incompatible (Gavrilenko and Sakhonenok, 1986). In this case Nb/Ta available for substitution in zircon is lowered. The other possibility is that the valency of Nb and Ta is not 5^+, but 3^+ or 4^+. In this case ionic radius of Ta is smaller than that of Nb (Shannon, 1976), and Ta could go preferentially into the Hf (Zr) site.
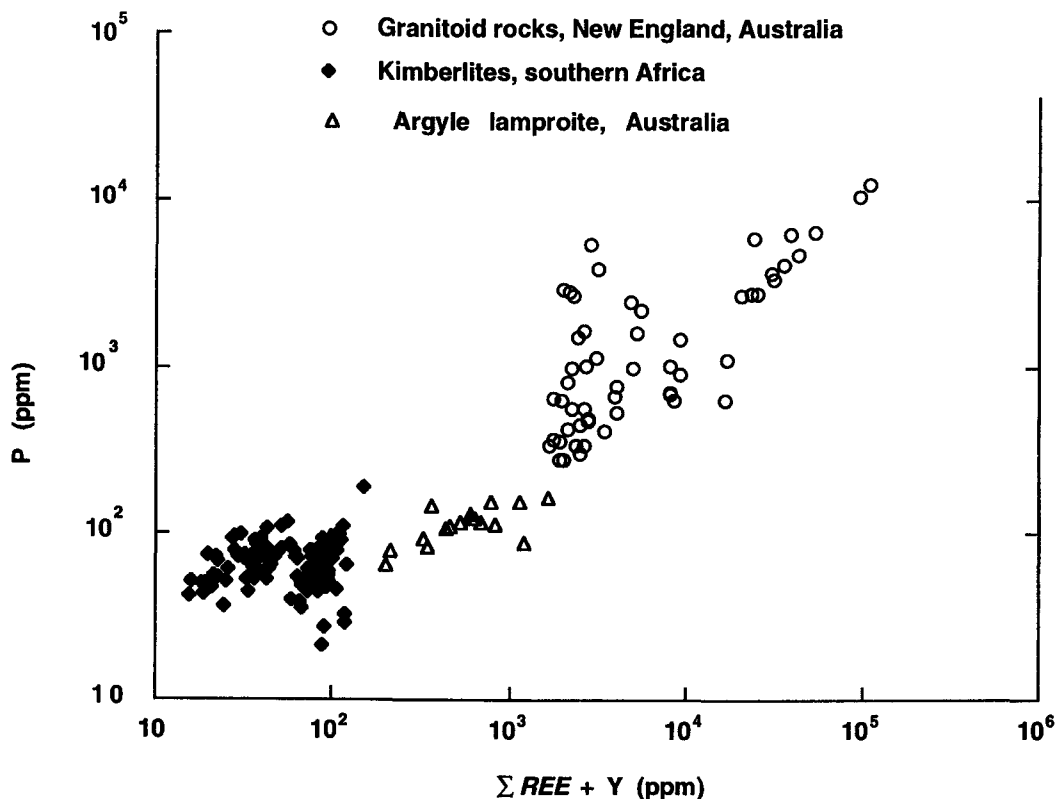
FIG. 4. Plot of *REE* + Y *vs.* P in zircons from different rock types, showing a positive correlation, suggesting the coupled substitution: $(REE, Y)^{3+} + P^{5+} = Zr^{4+} + Si^{4+}$.

Uranium and thorium contents of kimberlite zircons are low and never exceed 50–60 ppm for U and 10–15 ppm for Th; the more common range is from 6 to 20 ppm U and from 2 to 6 ppm Th (Fig. 2). Uranium concentrations obtained in this study show a good agreement with the fission-track data of Kresten *et al.* (1975) (Table 1), where zircon is homogeneous. Uranium contents of about 30 ppm or less are rarely encountered in zircons from other sources. Granitic zircons show uranium contents in the range 154–4116 ppm U (Ahrens *et al.*, 1967); values in the range 1000–2000 ppm U are most common (Kresten *et al.*, 1975). The average Th/U ratio calculated for the kimberlitic zircons is 0.29 ± 0.08. Most zircons with bluish CL colours have Th/U < 0.29 and those with yellowish CL typically have Th/U >0.29 (Fig. 5). Th/U ratio for kimberlitic zircons is slightly lower than for those from granitic rocks, which average 0.47 (Ahrens

et al., 1967), while the Th/U ratio for igneous rocks is approx 4. Ahrens *et al.* (1967) suggested that U^{4+} is preferentially accepted into the zircon structure (relative to Th^{4+}) because its ionic radius is closer to that of Zr^{4+} (Fig. 2).

The Rare Earth Element (*REE*) composition is the most distinctive feature of the kimberlite zircons (Figs 2,3). Total *REE* contents in all samples are less than 50 ppm. Light rare earth elements (*LREE*) show concentrations up to 2–3 ppm, but mainly less than 1 ppm and for La and often less than 0.5 ppm for Pr. Cerium shows a slight positive anomaly with usual values up to 1–2 ppm. Many studies have noted the marked predominance of heavy lanthanides in the zircon lattice. However, in the kimberlite zircons their contents seldom reach 10–12 ppm for Dy, Er and Yb, and 4–6 ppm for Gd, Ho and Lu. Europium commonly shows a very small negative anomaly and concentrations are usually less than 1 ppm.
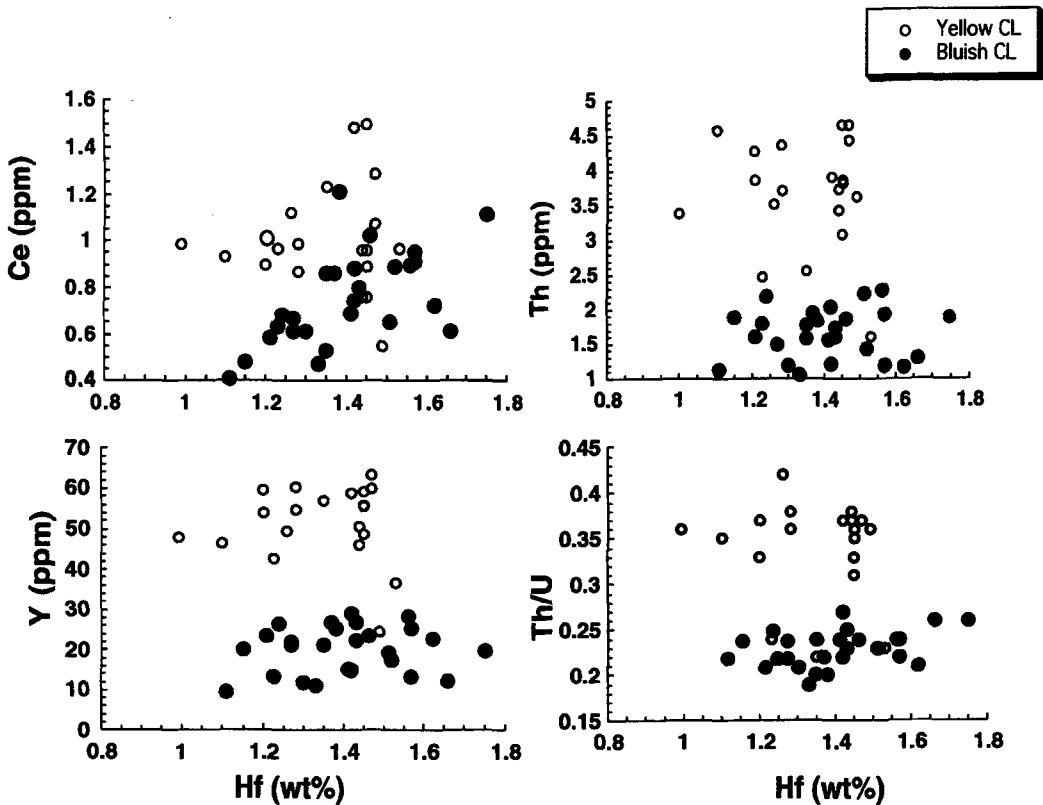
FIG. 5. Trace-element ratios for Monastery Mine zircons with yellowish and bluish CL colours.

Discussion of results

The analytical data, when compared with those for crustal zircons, demonstrate the distinctive trace element pattern of kimberlite zircons and provide well defined ranges for *REE*, Y, U, Th, P and some other trace elements (Fig. 2). The geochemical distinctiveness of the kimberlite zircons shows up most clearly in the *REE* distribution. Low total *REE* contents, no more than 50 ppm, contrast with crustal zircons, which may contain from several hundred to several thousand ppm *REE*. Although the results obtained here confirm the preferential entry of *HREE* into the zircon lattice, the chondrite-normalized *REE* patterns of kimberlite zircons are distinctive (Fig. 3):

(i) the slope of the *REE* patterns is not so steep, especially in the *HREE*, as for zircons from most crustal rock types (lower *HREE/LREE* ratios). To quantify the *REE* pattern slope, chondrite-normal-

ized $[Nd/Yb]_{cn}$ values have been calculated. They range from 0.01 to 0.1 with an average of 0.03 for kimberlitic zircons, while average $[Nd/Yb]_{cn}$ is 0.01 for zircons from granitoid rocks (Belousova,unpub. data), and 0.003 and 0.002 for samples 61308 and 91500 respectively;

(ii) the less pronounced Ce anomaly, connected with the presence of Ce^{4+}, indicates low redox conditions during crystallization;

(iii) the almost complete absence of a negative Eu anomaly contrasts with the crustal zircons, where negative Eu anomalies might be explained by preferential entry of Eu^{2+} ions into plagioclase.

Relatively low Y and P concentrations are connected with low *REE* contents and show a positive correlation over a wide range of zircon composition from different sources (Fig. 4; Belousova, unpub. data), suggesting a coupled substitution in zircon:

$$(REE, Y)^{3+} + P^{5+} = Zr^{4+} + Si^{4+}.$$
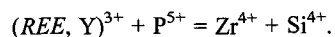
Kimberlite zircons break down into two separate groups with predominant yellow or bluish CL on this plot. However, it is not clear why the yellow-CL zircons with higher *REE* + Y values do not fit well into the overall pattern.

Figure 6 shows relations between Hf and Y, relative to the fields of zircon compositions typical of different rock types as defined by Shnyukov *et al.* (1989). Southern African kimberlitic zircons form a distinct field on this plot, out of the main trend defined by crustal zircons.

The range found for the U content is from 6 to 60 ppm (average 11 ppm), and consistent with determinations by Ahrens *et al.* (1967; 7.0–28.0

ppm U) and Kresten *et al.* (1975), who reported U values from 6.7 to 66 ppm with average of 16.5 ppm. In comparison, granitic zircons from the New England Batholith contain from 200 ppm to more than 1% of uranium (Belousova, unpub.-data).

There is a broad correlation between CL properties and trace-element composition. The averaged trace element data for zircons of bluish and yellowish CL colours are given in Table 1. Concentrations of *REE*, Y, U and Th are noticeably higher for zircons of yellow CL. In particular, this difference in contents reaches a factor of 2–3 for zircons from Monastery Mine (Fig. 5).
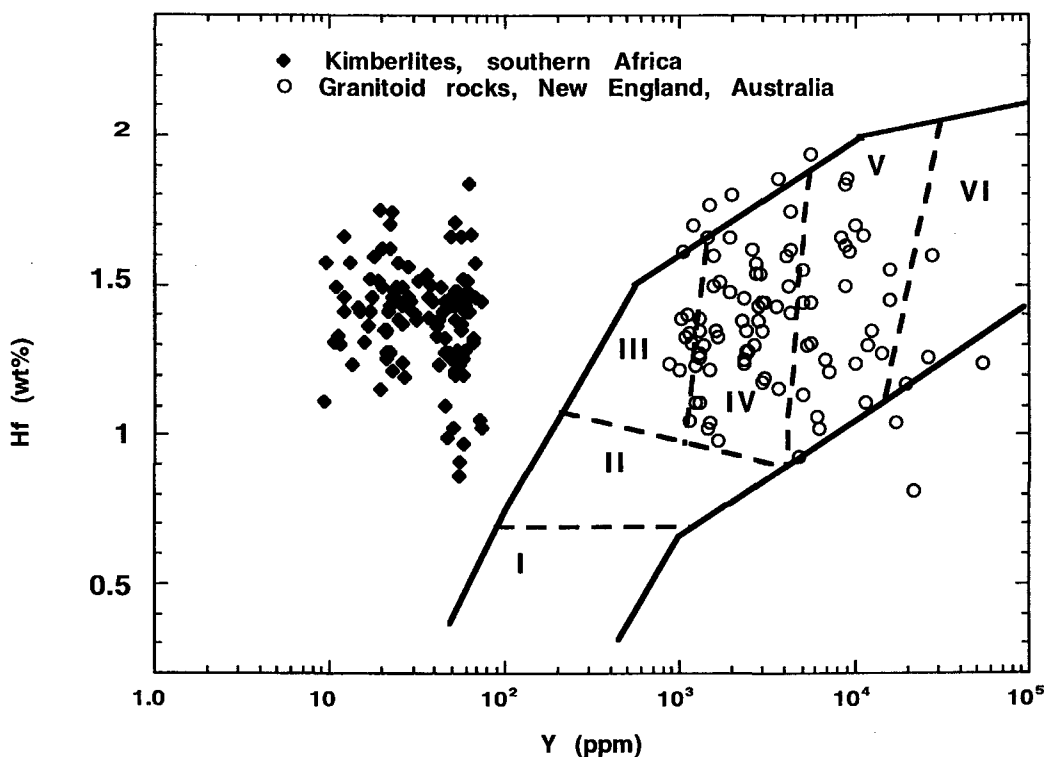
The fields of zircon composition from:
I - carbonatites;
II - alkali syenites and fenites;
III - calc-alkali basic rocks;
IV - calc-alkali felsic rocks;
V - ultra felsic granites and diaphthorites;
VI - gneisses.

FIG. 6. Relations between Hf and Y, relative to the fields of zircon compositions typical of different rock types, as defined by Shnyukov *et al.* (1989).

The luminescence characteristics of most minerals are determined by the presence of impurity cations in minor or trace amounts, substituting for lattice cations of similar ionic size (Marfunin, 1979). For zircon, which can incorporate a wide range of trace elements, the following ions are known to form luminescence centres: Ce^{3+}, Pr^{3+}, Nd^{3+}, Sm^{2+}, Sm^{3+}, Eu^{2+}, Eu^{3+}, Gd^{3+}, Tb^{3+}, Dy^{3+} and Yb^{3+}, as well as U^{6+}, Mn^{2+}, Fe^{3+}. Remond et al. (1996) studied the cathodoluminescence of synthetic zircon crystals by doping single rare-earth elements in the form of $(REE)^{3+}$ ions with addition of phosphorous to obtain charge balance. They concluded that each individual REE activator is responsible for specific CL colours: Ce, Gd and Nd for blue, Dy for blue-green, Tb for yellow-green and Eu for orange colours. Furthermore, the intensity of characteristic cathodoluminescence emission is a function of the concentration of the corresponding REE activator and P.

However, crustal zircons examined so far exhibit mainly dull yellowish CL colours. One explanation of this phenomenon may be that zircon incorporates a number of element-activators which give a mixture of colours. Another explanation of the dominant yellowish CL can be deduced from the study by Remond et al. study of an undoped synthetic zircon (without addition of REE and P), which shows yellow CL; this colour was interpreted as associated with lattice defects. This suggests that the generally high levels of trace-element impurities (mostly with ionic radii larger than the Zr–Hf site; Fig. 2) in most crustal zircons can create strain and lattice defects, which are responsible for yellowish CL colours. In contrast, kimberlite zircons have predominantly bluish CL colours. The low concentrations of the whole range of trace elements in these zircons probably leads to a much lower density of lattice defects, and this in turn may allow the direct excitation of REE^{3+} ions, most of which cause bluish CL hues.

The low levels of REE, as well as low concentrations of U, Th, Y, P and other trace elements, suggest that these zircons originated from primitive, deep-seated sources distinct from those associated with most known crustal zircons. The relatively large size of the zircon crystals and the relatively homogeneous internal structure of most of them suggest crystallization under stable conditions.

The bluish cathodoluminescence colours, directly connected with low trace-element concentration, can serve as a rapid method for preliminary identification of most kimberlite zircons during diamond exploration. LAM-ICPMS analysis of such grains, and of large grains with yellowish CL, can then be used to verify whether they show the distinctive compositional patterns found by this work.

Acknowledgements

References

Ahrens, L.H., Cherry, R.D. and Erlank, A.J. (1967) Observations on the Th-U relationship in zircons from granitic rocks and from kimberlites. Geochim. Cosmochim. Acta, 31, 2379–87.

Gavrilenko, V.V. and Sakhonenok, V.V. (1986) Basis of Geochemistry of Rare Lithophylic Metals. Leningrad University, 1–172 (in Russian).

Guo, J., O'Reilly, S.Y. and Griffin, W.L. (1996) Zircon inclusions in corundum megacrysts I: trace element geochemistry and clues to the origin of corundum megacrysts in alkali basalts. Geochim. Cosmochim. Acta, 60, 2347–63.

Jensen, B.B. (1973). Patterns of trace element partitioning. Geochim. Cosmochim. Acta, 37, 2227–42.

Kabanova, Ye.S., Skosyrova, M.V. and Solodov, N.A. (1982) Geochemistry and Mineralogy of Tantalum and Niobium. Moscow, 1–175 (in Russian).

Krasnobayev, A.A. (1979) Mineralogical-geochemical features of zircons from kimberlites and problems of their origin. Internat. Geology Rev., 22, 1199–209.

Kresten, P., Fels, P. and Berggren, G. (1975) Kimberlite zircons – a possible aid in prospecting for

kimberlites. *Mineral. Deposita* (Berl.), **10**, 47–56.

Lyakhovich, V.V. (1996) Zircons in diamond-bearing rocks. *Trans. (Doklady) Russian Acad. Sci./Earth Sci. Sections*, **347**, 179–99.

Marfunin, A.S. (1979) *Spectroscopy. Luminescence and Radiation Centers in Minerals* (Translated by V.V. Schiffer). Springer-Verlag, Berlin, Heidelberg, New-York, 1–347.

Moore, R.O., Griffin, W.L., Gurney, J.J., Ryan, C.G., Cousens, D.R., Sie, S.H. and Suter, G.F. (1992) Trace element geochemistry of ilmenite megacrysts from the Monastery kimberlite, South Africa. *Lithos*, **29**, 1–18.

Norman, M.D., Pearson, N.J., Sharma, A. and Griffin, W.L. (1996) Quantitative analysis of trace elements in geological materials by laser ablation ICPMS: instrumental operating conditions and calibration values of NIST glasses. *Geostandards Newsletter*, **20**, 247–61.

Remond, G., Blanc P., Cesbron, F., Ohnenstetter, D. and Rouer, O. (1996) Cathodoluminescence of rare earth doped zircons: Part II: relationship between the distribution of the doping elements and the contrasts of CL images. *Scanning Microscopy*, suppl. **9**, 57–76.

Shannon, R.D. (1976) Revised effective ionic radii and systematic studies of interatomic distances in halides and chalcogenides. *Acta Crystallogr.*, **A32**, 751.

Shnyukov, S.E., Cheburkin, A.K. and Andreev, A.V. (1989) Geochemistry of wide-spread coexisting accessory minerals and their role in investigation of endogenetic and exogenetic processes. *Geol. J.*, **2**, 107–14 (in Russian).

Taylor, S.R. and McLennan, S.M. (1985) *The Continental Crust: its Composition and Evolution*. Blackwell Sci. Publ., Oxford.

Wiedenbeck, M., Alle, P., Corfu, F., Griffin, W.L., Meier, M., Oberli, F., Von Quart, A., Roddick, J.C. and Spiegel, W. (1995) Three natural zircon standards for U-Th-Ph, Lu-Hf, trace element and REE analyses. *Geostandards Newsletter*, 19, 1–23.